A 19-ELEMENT SHOCK SENSOR ARRAY FOR BI-DIRECTIONAL SUBSTRATE-PLANE SENSING FABRICATED BY SACRIFICIAL LIGA

Shamus McNamara and Yogesh B. Gianchandani[1]
Department of Electrical and Computer Engineering, University of Wisconsin, Madison, USA

ABSTRACT

The design, fabrication and testing of a micromachined shock sensor array is described. The sense elements are cantilevers which deflect parallel to the substrate and close a switch when a threshold acceleration is detected. Criteria for their dimensional optimization are presented. The dynamic range for the array is 10 g to 150 g, with a resolution of 10 g. Provisions for electrostatic self-testing are included. With triple redundancy at the 20 g and 100g thresholds, the total area occupied is <21 mm^2. Measurement results are presented for arrays fabricated by the sacrificial LIGA process. Electrostatic self-testing shows that actuated with a 100V pulse, a dynamic self-test gives a typical closure time of less than 1 ms.

Keywords: accelerometers, shock sensors, LIGA

I. INTRODUCTION

Accelerometers are one of the largest applications of micromechanics and have been the subject of active research for more than two decades [1]. Shock sensors are accelerometers which are designed to respond to threshold levels of acceleration [2-9]. The typical design includes a proof mass and a flexible suspension. At a pre-selected level of acceleration, the deflection of the proof mass will typically contact an electrical switch, much like a relay. Since each sense element triggers at a single threshold, it is necessary to use arrays to service a wide dynamic range. The discretized output that is generated permits these devices to operate with a relatively simple interface circuit, which can be designed to have minimal power dissipation [9]. This permits long term operation from a small battery. The intended application for the devices presented here is to wake up an environmental monitoring system when a shock is detected. The system, which monitors temperature, pressure, humidity, and a number of other variables, is normally in a sleep mode to preserve battery life. Other potential applications for shock sensors include air-bag deployment, munitions arming, monitoring seismic activity, and monitoring fragile shipments.

In most implementations of shock sensors, the proof mass returns to its rest position once the acceleration is removed. However, devices in which the deflection is latched have also been reported [2,3]. This "memory" can be useful for certain applications, but may compromise sensitivity and re-usability.

Most shock sensors reported in the past have detected out-of-plane accelerations. Substrate-plane sensing frequently simplifies mounting and alignment. It also simplifies bi-directional sensing (i.e. along the positive and negative direction of the sense axis) because electrodes can be in the same plane as the proof mass and only one structural and electrical layer is required. There is only one report of a substrate-plane sensing device in the past, but it targets very high g-forces [4].

A persistent challenge for shock sensors has been closing and opening the electrical contact [7,9]. When the proof mass is very small, its momentum may fail to break though surface films that may inadvertently form on the electrical contact. Also, if the suspension is too weak, forces established during contact may prevent the retraction of the proof mass.

This paper presents a 19-element shock sensor array for 10 g to 150 g acceleration thresholds that provides substrate-plane sensing and detects both positive and negative accelerations. Provisions for electrostatic self-testing are included. Using LIGA technology [10], metal suspensions and proof masses as large as 0.2 milligrams are fabricated. This design and implementation circumvents many of the challenges that have been encountered in the past. Although LIGA has been used to create an accelerometers [11], it has not been used for a threshold accelerometer in the past.

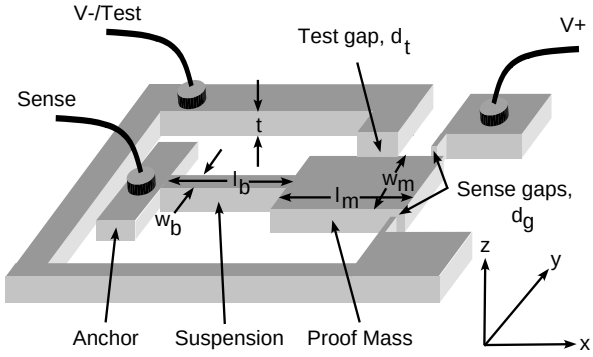

Fig. 1: Schematic of a single sense element showing both pick-off electrodes and the self-test electrode.

[1] Address: 1415 Engineering Dr., UW-Madison, WI 537016-1691, USA; Tel: (608) 262-2233; Fax: 262-1267; E-mail: yogesh@engr.wisc.edu

II. DESIGN

A schematic of a single sense element is shown in Fig. 1. The proof mass at the end of a cantilever moves when subject to an acceleration. When the mass closes the sense gap it makes electrical contact with one of the two nearby pick-off electrodes, allowing detection of a threshold acceleration. The sense element is measured by reading the voltage on the proof mass, which is biased to ground through a resistor. The pick-off electrodes are biased with voltages of opposite polarity in order to determine the direction of acceleration. A self test electrode, shared with the negative pick-off electrode permits the proof mass to be deflected electrostatically when a large enough voltage is applied. The gap between the test electrode and the mass is relatively large, so the motion of the proof mass is stopped by the negative pick-off electrode and it never comes into contact with the test electrode.

If the suspension is weightless and the proof mass rigid, the acceleration threshold is given by [1]:

$$a_t = \frac{E w_b^3 d_g}{\rho w_m l_m l_b}\left[\frac{1}{4l_b^2 + 9l_b l_m + 6l_m^2}\right] \quad (1)$$

where E is Young's modulus, ρ is the density, w_b and l_b are the width and length of the suspension, w_m and l_m are the width and length of the proof mass, and d_g is the sense gap. In order to verify the validity of this equation, a non-linear finite element analysis (FEA) was performed for the 10 g and 150 g sense elements using ANSYS with a solid92 element type. This analysis agrees with equation (1) to within 1% over the expected deflection range.

The resonant frequency, which determines the bandwidth because there is little damping, is [1]:

$$\omega_n \cong \sqrt{\frac{w_b^3 E}{12\rho l_m w_m l_b^3}} \bullet \frac{2 + 6f + f^2}{0.666 + 4f + 10.5f^2 + 14f^3 + 8f^4} \quad (2)$$

where $f=l_m/2l_b$. This may be rewritten in terms of the threshold acceleration as:

$$\omega_n \cong \sqrt{\frac{a_t}{12 d_g}} \sqrt{\frac{8 + 50f + 160f^2 + 162f^3 + 24f^4}{0.666 + 4f + 10.5f^2 + 14f^3 + 8f^4}} \quad (3)$$
$$= g(f)\sqrt{\frac{a_t}{12 d_g}}$$

The function g(f) is plotted in Fig. 2. For a given threshold acceleration and sense gap, the resonant frequency is maximized at f=0.3.

For a fixed total length L and given threshold acceleration, the tip deflection is maximized when the beam length is 44.64% of the total length L. Figure 3 is a normalized plot showing the relationship between the tip deflection and the beam length. Since the resonant frequency is optimized for a beam length of 62.5% of the total length, a trade-off must be made during the design process.

The lengths selected for the proof mass and beam are 420 μm and 600 μm, respectively, for all sense elements. This results in a near optimal resonant frequency. The cantilever beam width is 9 μm for the 10 g – 40 g sense elements and 10 μm for the higher g sense elements. The mass widths are varied to set the sense element to the correct sensitivity. The thickness, typically 100-300 μm, does not matter for the primary design criteria, but it does impact the z-axis sensitivity. The test electrodes are all 245 μm wide in order to facilitate comparison between sense elements. They are designed not to contact the proof mass, thus avoiding a large current flow that can fuse the contacts [7]. Figure 4 shows the proof mass widths and cantilever beam widths used in this design. The pin count is minimized by combining all the positive pick-off electrodes and all the negative pick-off electrodes, and by sharing the test electrode leads with the latter. Only the proof masses are individually wired.

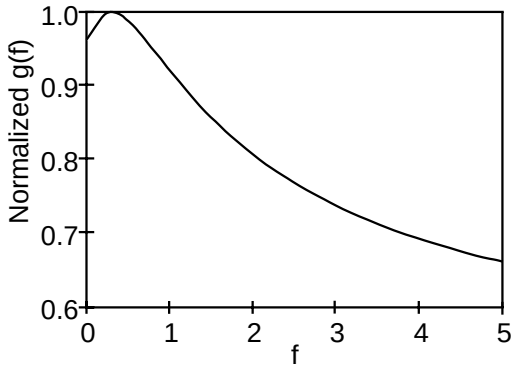

Fig. 2: The device bandwidth peaks at f≈0.3.

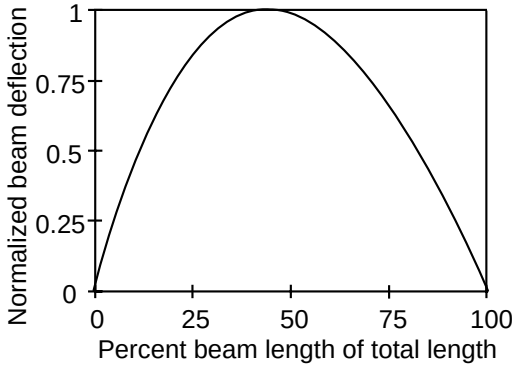

Fig. 3: Optimization of tip deflection given a constrained total length $L=l_m+l_b$. The optimum beam length is 44.64% of L.

III. FABRICATION AND TEST RESULTS

The device is fabricated using a standard LIGA process to create Ni and Ni/Fe structures attached to the substrate [10]. Gold is then electroplated over the nickel to reduce the contact resistance. Finally, a copper sacrificial layer is time etched to free the proof mass and suspension beam. The anchor supports are sufficiently large that they are not freed during the timed sacrificial etch. Wire bonding during packaging is done directly to the anchors. Figure 5 is an SEM of the fabricated die of the 19-element shock sensor. The floor plan was designed for convenient wire-bonding when inserted in a dual in-line (DIP) package. The footprint of the die is 3680 µm x 5670 µm. Figure 6 shows two SEM images of the same die providing details of the device structure.

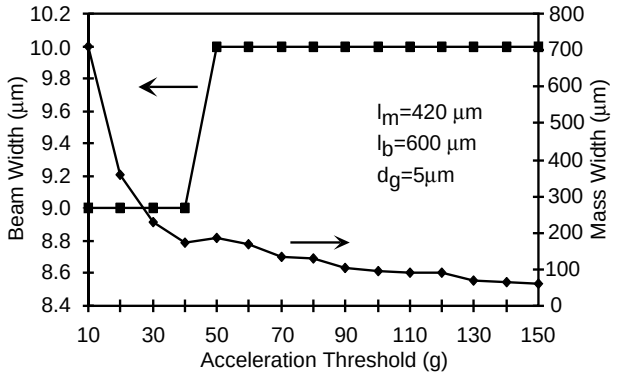

Fig. 4: Dimensions selected for all 15 sense elements.

Both static and dynamic self-testing may be performed. The static test measures the pull-in voltage required to deflect the proof mass and trigger electrical contact. The dynamic test measures the time required for the proof mass to contact the detection electrode after a step voltage is applied to the test electrode. Although simpler, the former test cannot discriminate between different mass sizes. The dynamic self-test is more complete, but requires a more challenging interpretation. The equation to find the actuation time is a non-linear second-order differential equation, but it is easily evaluated numerically.

The pull-in voltage required for static testing of the sense element is calculated by equating the spring force and the electrostatic force, and then solving for the displacement. This is a cubic equation and the solution of interest is where there are three real roots, two of which are repeated. Assuming that the proof mass deflection is small and that the test gap is constant, the pull-in voltage is:

$$V_{crit} = \sqrt{\frac{8\rho d_t^3 l_m a_t w_m}{27\varepsilon_0 l_t d_g}} \qquad (4)$$

where l_t is the test electrode length and d_t is the test gap. The static self-tests were carried out by ramping the voltage on the test electrode and electrically measuring when the proof mass makes contact with the pick-off electrode. The pick-off electrode was connected to a 5V bias, while the proof mass was grounded through a large resistor to minimize current flow. Figure 7 shows optical images of the proof mass before and during self-test actuation. Figure 8 shows two sample measurements.

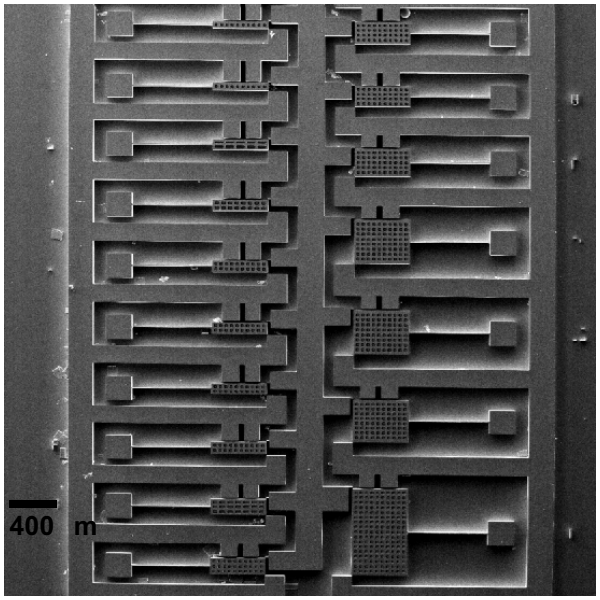

Fig. 5: SEM of fabricated shock sensor array.

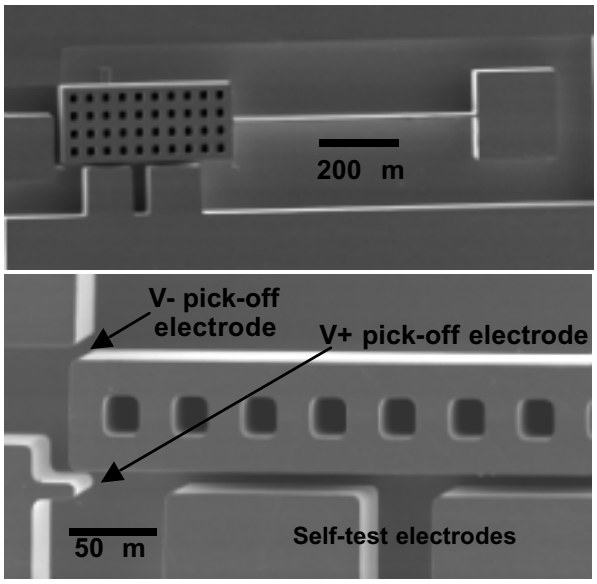

Fig. 6: SEM images showing entire sense element (upper) and close-up of proof mass with pick-off and self-test electrodes (lower).

Fig. 7: Optical images showing a proof mass before (left) and after (right) static self-test actuation.

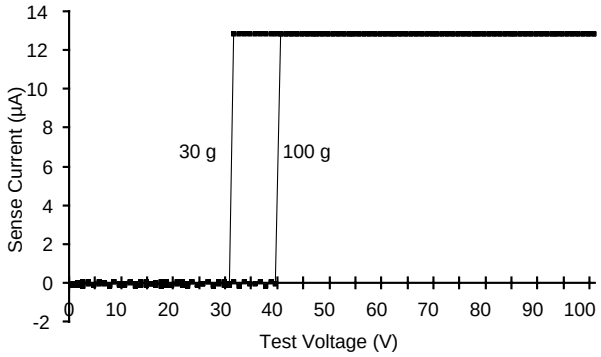

Fig. 8: Sample static self-test measurements for the 30g sense element and the 100 g sense element.

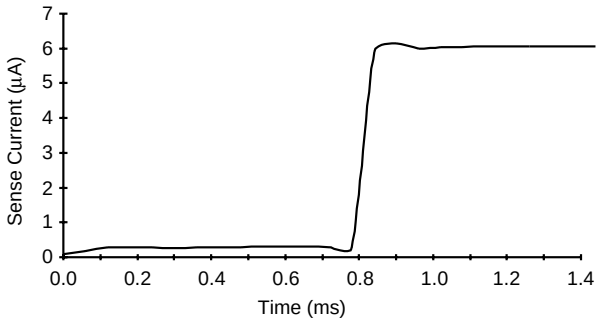

Fig. 9: Dynamic self-test measurement for the 100g sense element.

Dynamic self-tests were performed using the same test setup as for the static self-test, except the voltage was not ramped. Instead, the time interval is measured between application of a 100V step and when electrical contact was established between the proof mass and pick-off electrode (Fig. 9).

Reliability testing has been initiated for devices that were assembled in a DIP and inserted in a battery-operated circuit assembled on a breadboard. The unit momentarily lights an LED when subjected to an external impact. As of the time of this writing, the device has been working for three weeks without fail.

IV. CONCLUSION

A compact array of shock sensors was developed for bi-directional sensing in the plane of the substrate. Criteria for dimensional optimization were presented. Devices were fabricated from electroplated Ni and Ni/Fe covered with a thin layer of Au. Electrostatic self-testing results of both pull-in measurements and transit time measurements were presented.

Yield analysis at this point in the development of the shock sensor array indicates that the elements with smaller proof masses are more robust and more able to survive mishandling, as should be expected. In future designs the larger proof masses will be better constrained to limit their motion in the release process and in subsequent handling and testing. In particular, elements will be added to prevent the rotation of the proof mass, which is periodically observed in the present implementation.

ACKNOWLEDGEMENTS

This effort was supported in part by Canopus Systems, Inc., through US Army Aviation and Missile Command (AMCOM) contract DAAH01-00-C-R104. The facilities used for this research included the Wisconsin Center for Applied Microelectronics (WCAM), and the NSF-supported Synchrotron Radiation Center (SRC) at the University of Wisconsin, Madison.

REFERENCES

[1] L.M. Roylance, J.B. Angell, "A Batch-Fabricated Silicon Accelerometer," *IEEE Trans. Elec. Dev.*, ED-26, 1979, pp. 1911-17

[2] R. Ciarlo, "A Latching Accelerometer Fabricated by the Anisotropic Etching of (110) Oriented Silicon Wafers," *J. Micromech. Microeng.*, v. 2, 1992, pp. 10-13

[3] X.-Q. Sun, S. Zhou, W. Carr, "A Surface Micromachined Latching Accelerometer," *Transducers '97*, pp. 1189-92

[4] P.F. Man, C.H. Mastrangelo, "Surface Micromachined Shock Sensor for Impact Detection," *Solid-State Sensor and Actuator Workshop*, Hilton Head, 1994, pp. 156-159

[5] W. Frobenius, S. Zeitman, M. White, D. O'Sullivan, R. Hamel, "Microminiature Ganged Threshold Accelerometers Compatible with Integrated Circuit Technology," *IEEE Trans. Elec. Dev.*, ED-19, 1972, pp. 37-40

[6] C. Robinson, D. Overman, R. Warner, T. Blomquist, "Problems Encountered in the Development of a Microscale g-switch …," *Transducers '87*, pp. 410-413

[7] Y. Loke, G. McKinnon, M. Brett, "Fabrication and characterization of silicon micromachined threshold accelerometers," *Sensors & Actuators A*,. 29, 1991, pp. 235-240

[8] J.S. Go, Y.-H. Cho, B.M. Kwak, "Acceleration Micro-switches with Adjustable Snapping Threshold," *Transducers '95*, pp. 691-694

[9] A. Selvakumar, N. Yazdi, K. Najafi, "Low Power, Wide Range Threshold Acceleration Sensing System," *IEEE MEMS '96*, pp. 186-191

[10] H. Guckel, "High-Aspect-Ratio Micromachining via Deep X-Ray Lithography," *Proc. IEEE*, 1998, pp. 1586-93

[11] C. Burbaum, J. Mohr, P. Bley, W. Ehrfeld, "Fabrication of Capacitive Acceleration Sensors by the LIGA Technique," *Sensors & Actuators A*, v. 25-27, 1991, pp. 559-63